Texture and microstructure of lath martensite

H. Welland, H.J. Bunge, Institut für Metallkunde und Metallphysik,

TU Clausthal, FRG

L.M. Matthews, Physical Metallurgy Division, Mintek, Randburg, South Africa

Introduction

Although studies on the texture transformation from austenite to martensite have been reported (1), little is known of the texture of lath martensite in dual phase ferrite and lath martensite steels. This is largely due to the difficulty in resolving the X-ray diffracted peaks of the ferrite and lath martensite that forms in the low carbon steels. Orientations of individual martensite packets and ferrite grains were measured using a technique to evaluate Kikuchi patterns on-line in a transmission electron microscope (TEM). Thus, the texture development in ferrite and martensite could be determined seperately. It was also possible to calculate the misorientation distributions between neighbouring martensite packets and between martensite and ferrite.

Experimental

For the formation of Kikuchi patterns in a TEM it is essential that the part of the specimen under investigation illuminated by the electron beam is virtually perfect. Using microbeam electron diffraction with spot sizes down to 120 nm it was possible to find such regions even in deformed martensite packets. The orientations of individual crystals were then calculated in Eulerian angles by the on-line evaluation of the Kikuchi patterns (2). Orientation distribution functions (ODF) were obtained by superposing a Gaussian peak with a spread of 10° over each single orientation and by making use of the series expansion method (3). The so determined ODFs were analyzed. Misorientation distribution functions (MODF) were obtained by expressing also the misorientations of neighbouring crystals in Eulerian angles and applying the same mathematics for the MODF as for the ODF (4).

Two commercial low carbon steels were investigated, a cold and a hot rolled one. *Steel A* is a dual-phase steel with 0.05 wt-% C, 2.55 wt-% Mn, 0.44 wt-% Si and 0.030 wt-% Al. After cold rolling with a reduction degree of 67% this steel was open-coil annealed in the intercritical region at 730 °C for 3 h and then cooled down with 150 °C/min to RT. In this condition (as-received) the material consists of ferrite with 20 vol-% lath martensite. The ODF, MODF and OCF of Steel A were determined in the as-received condition and after a tensile test with 14% elongation. In each condition 210 single martensite orientations were determined in several samples. *Steel B* is a chromium-bearing alloy (12 wt-% Cr, 0.023 wt-% C, 0.58 wt-% Ni and 0.39 wt-% Ti). It enters the two-phase austenite-ferrite region above 780 °C. The maximum austenite content of 80% is obtained at 1050 °C. Due to the chromium content of the steel the austenite transforms to martensite on air-cooling with an Ms temperature of approximately 550 °C. For this experiment the material was hot rolled in the temperature range 1050 to 800 °C which is within the two-phase austenite-ferrite region. After total reductions of 20% and 80% respectively, the material was allowed to air-cool. In steel B 50 single martensite orientations were determined for both conditions.

Results

The microstructure of *steel A* in the as-received condition consists of polygonal ferrite with 20% islands of lath-martensite (figure 1a). Retained austenite or other phases could not be detected neither by X-ray diffraction nor by electron microscopy. In each martensite island many differently orientated laths are observed (Figure 1b). The dislocation density in the ferrite matrix increases at phase boundaries as a result of the austenite-martensite transformation. After the tensile-test, the alignment of the martensite particles changes relative to the tensile direction. Furthermore, the aspect ratio of individual islands, measured in the longitudinal plane of the specimen, changes during deformation. The aspect ratio is here defined as the maximum length of individual martensite islands over their minimum width. Considering that the aspect ratio consists of two parts, one is due to the deformation of the martensite and one to the alignment of particles out of the matrix into the observed plane, the deformation degree of the martensite can be estimatet to about 12%.

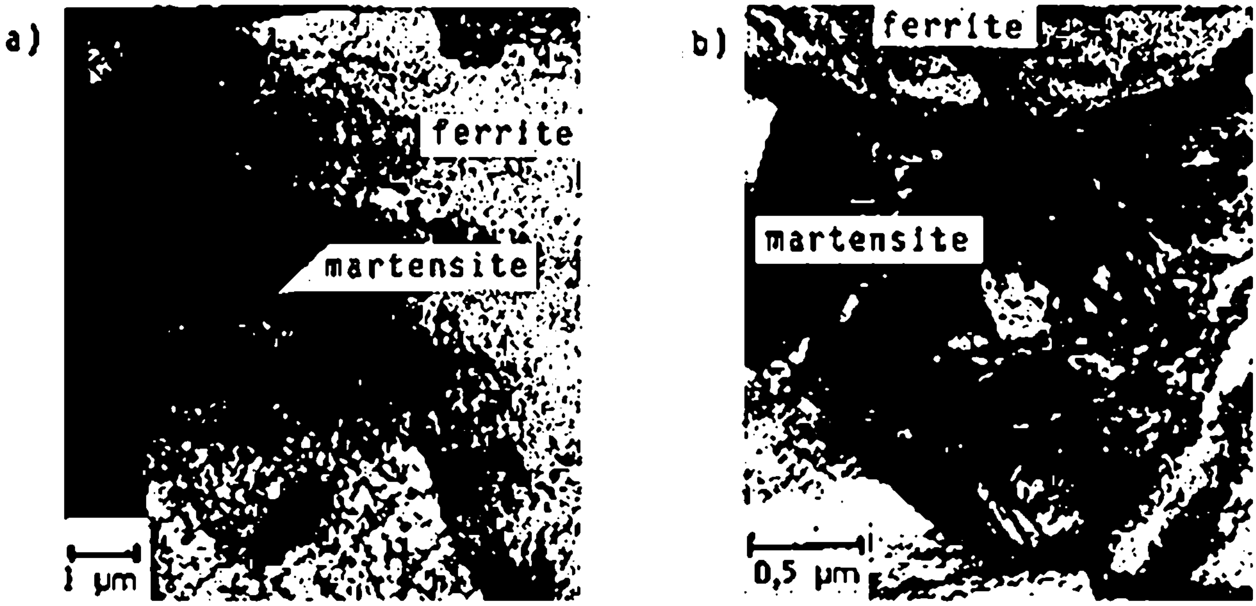

Figure 1: a,b) Microstructure of steel A (as-received)

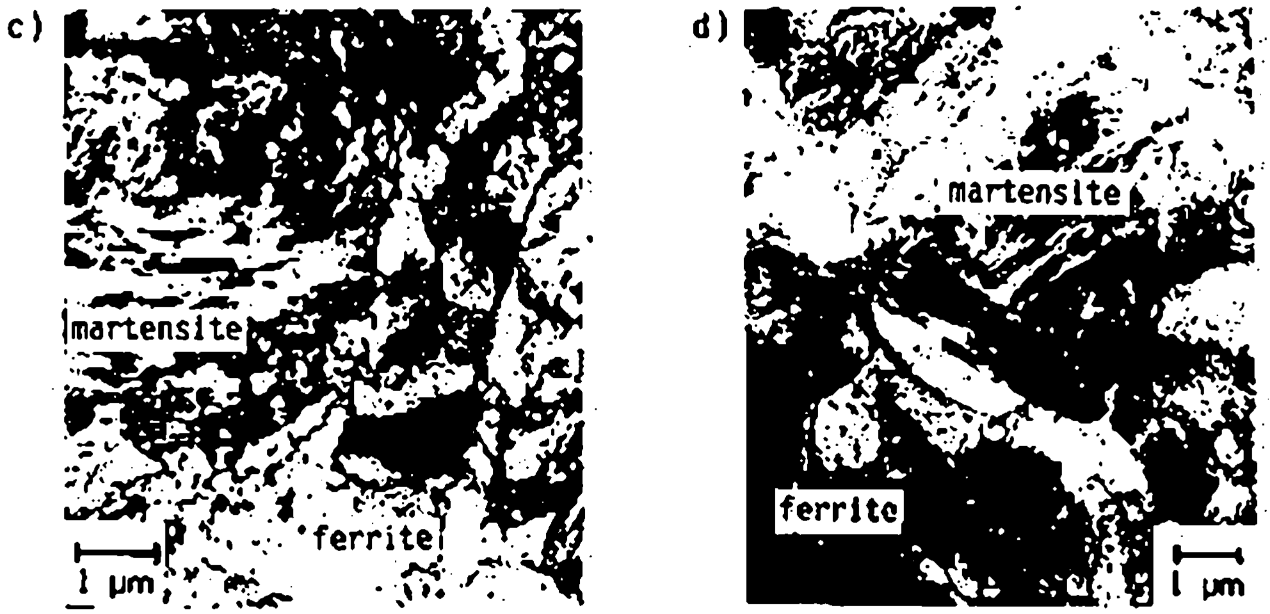

c,d) Microstructure of steel B reduced by 20% (c), by 80% (d)

As a consequence of the preceeding austenite-martensite transformation, the texture of the martensite in the as-received condition is weak. It consists of two components (Figure 2a), one (I) with an orientation path in normal direction (ND) from (101) to (211), while the rolling direction shifts around <111>. The second component (II) is in rolling direction (RD) close to <111> and covers in ND a wide range from (221) over (231) to (111). After tensile deformation the texture (Figure 2b) consists of a (111)[uvw]-fibre (III) and an orientation path (IV) from (211) to (210) in ND and in tensile direction from [113] to [135].

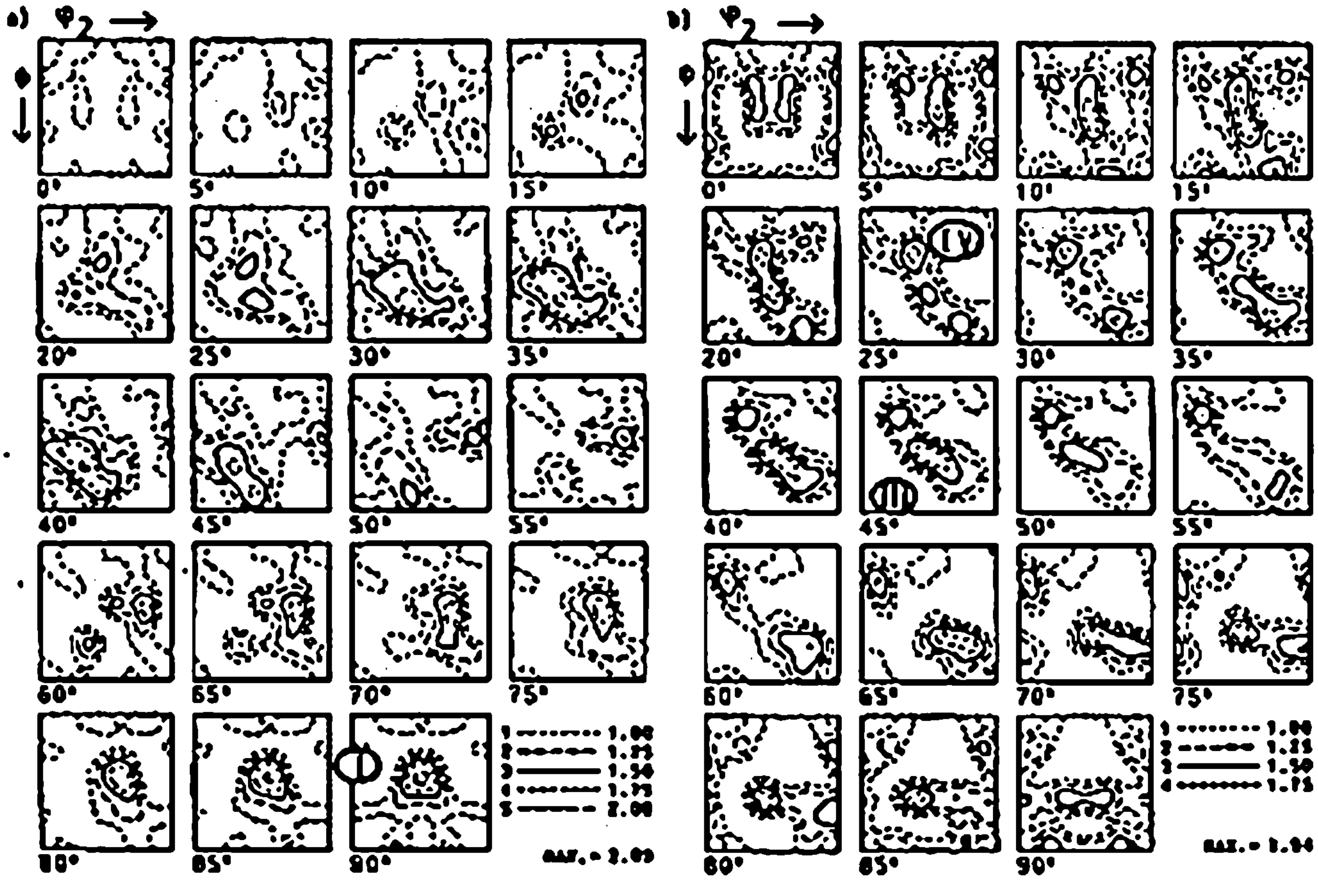

Figure 2: ODF of martensite for steel A
a) as-received b) 14% tensile-deformation

The textures of ferrite in steel A correspond for the as-received material to recrystallized (Figure 3a) and after the tension-test to deformed (Figure 3b) low-alloyed, low-carbon steel, both described by fibres with different distances from the (111)[uvw]-fibre and with different positions of their maxima on these fibres.

The orientation relationships between martensite laths in the as-received condition show Σ 3 and Σ 17 coincidences and a Bain relationship which can be described by a rotation of 45° around <100> (Figure 4a). Between neighbouring ferrite-martensite crystals no coincidences are found. The two maxima in the distribution are related to rotations I) of 47° around <411> and II) of 7° around <110> (Figure 4b). After deformation the orientation relationship between ferrit and martensite has changed. It shows now low-angle misorientations (φ_1=Φ=φ_2=0°) and Σ 3 coincidences (Figure 4c).

Due to the hot rolling of *steel B* a banded structure of ferrite and martensite was obtained with approximately 50% martensite. The microstructure of the material reduced by 20 and 80% is shown in figure 1 c,d. The ferrite and martensite bands

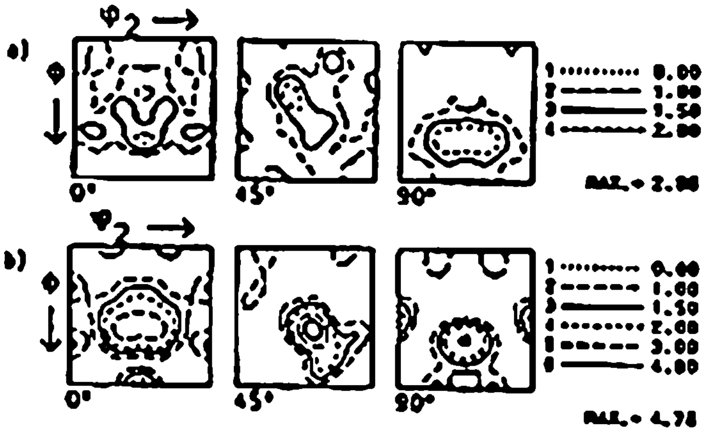

Figure 3: ODF of ferrite for steel A

a) as-received

b) 14% tensile-deformation

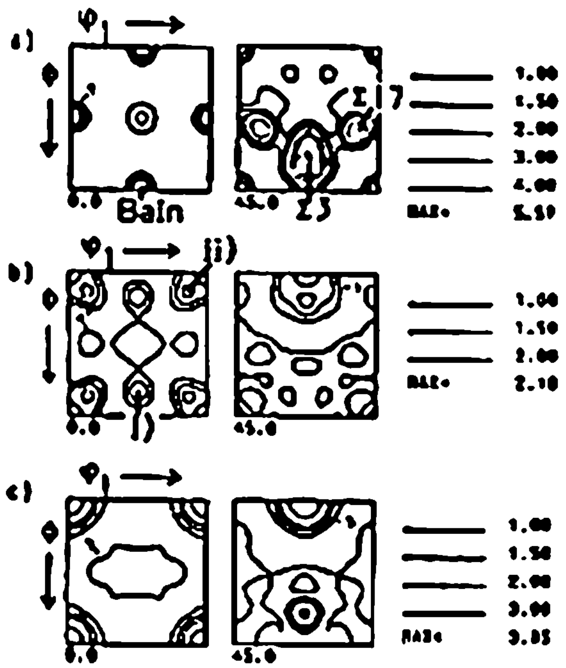

Figure 4: Orientation relationship between

a) martensite packets (as-received)

b) martensite-ferrite (as-received)

c) martensite-ferrite (after tensile-test)

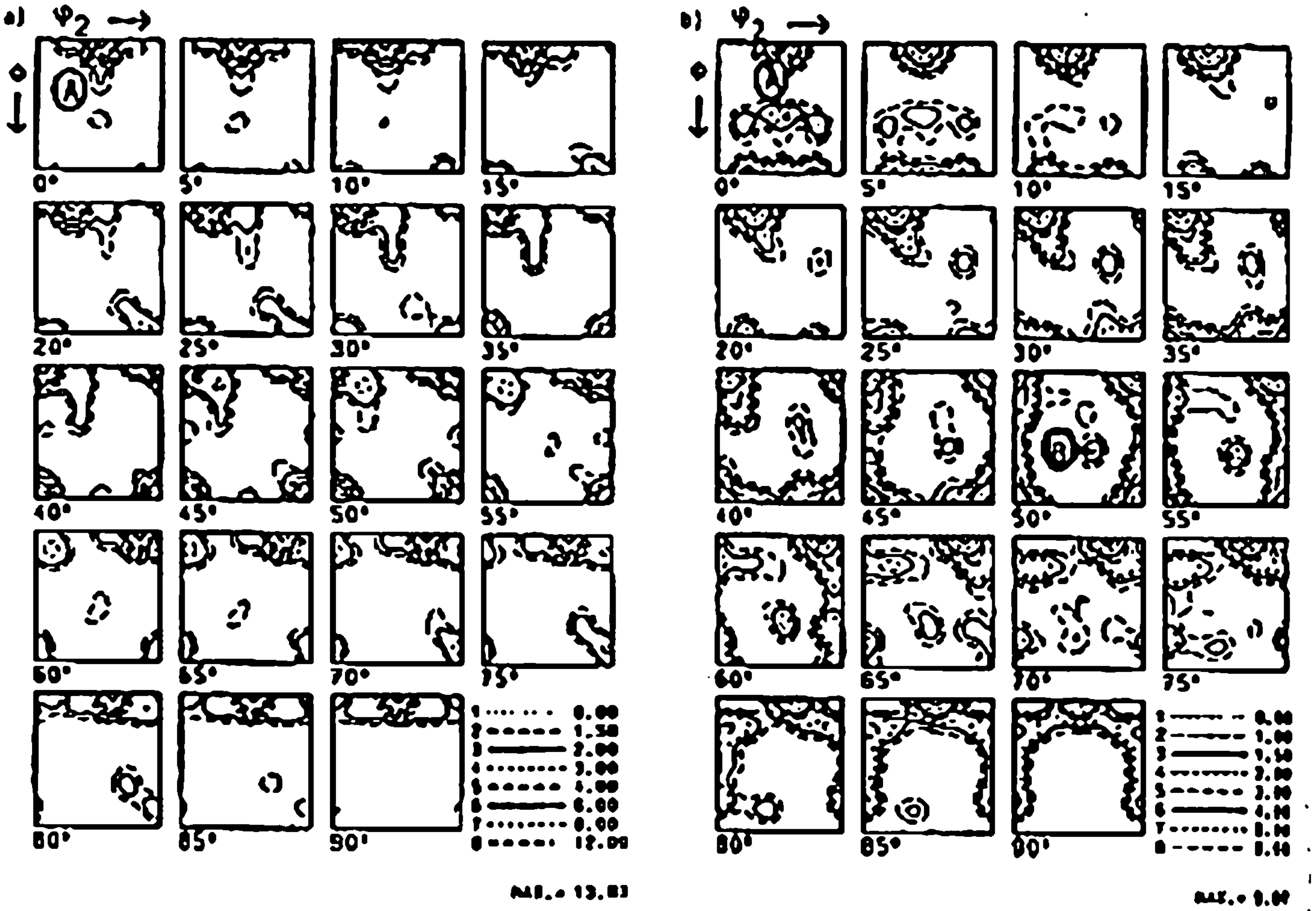

Figure 5: ODF of martensite for steel B reduced a) by 20% b) by 80%

are narrower for the reduction of 80%. Although the packets formed within the prior elongated austenite areas, the laths formed in different packets were randomly orientated when observed morphologically. As an example the laths within the packets on either side of the ferrite band (Figure 1c) are seen to lie at right angles to each other.

Orientation measurements of individual laths within a packet gave very little differences in orientation between different laths. The texture results therefore represent the orientation of different martensite packets. Figure 5 a,b give the ODF for the martensite of steel B reduced by 20 and 80% respectively. For 20% reduction the strongest texture (A) is represented by (100) planes parallel to the rolling plane and <1$\bar{1}$0> direction parallel to the rolling direction (represented as (100)[$\bar{1}\bar{1}$0]), with a spread to (100)[$\bar{1}$30]. In the case of 80% reduction the strongest orientation (A) is again the (100)[1$\bar{1}$0] orientation. There is also a weak orientation path (B), which can be described by a rotation starting from (132)<310> through the orientations (122)<201> and (111)<101> to (221)<114>.

The texture of the ferrite phase in steel B was also determined for the two reductions shown. For 20% reduction the ferrite (Figure 6a) was found to form with a texture best described by path (112)<110> to near (112)<211> and another (111)<2$\bar{1}$3> to (111)<1$\bar{1}$2>. For 80% reduction the ferrite texture (Figure 6b) was very similar to the martensite texture with a strong (100)<011> texture and a weak (111)<110> texture.

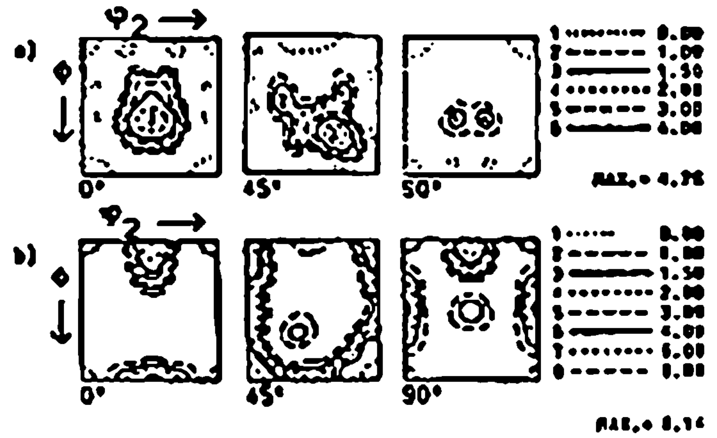

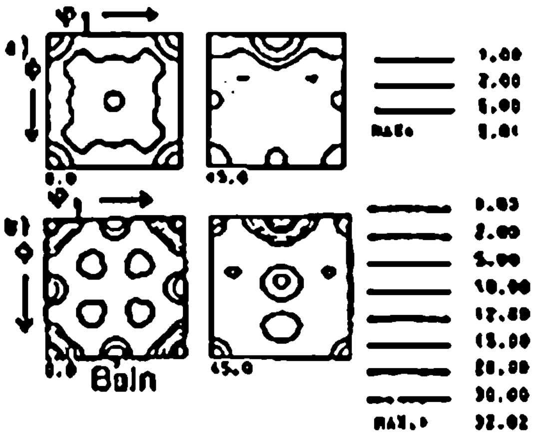

Figure 6: ODF of martensite for steel B reduced a) by 20% b) by 80%

Figure 7: Orientation relationship between a) martensite-ferrite (after 80% hot-rolling) a) martensite packets (after 80% hot-rolling)

The orientation relationships between ferrite and the martensite were determined for the alloy reduced by 80% and were found to have a strong relationship between the phases. This is expected from the measured texture. Both the ferrite and martensite have strong (100)<011> textures which result in low-angle misorientations (Figure 7a). The relationship between martensite packets was also calculated and was also found to have predominantly low-angle misorientations (Figure 7b). This would arise from the strong texture measured in the martensite. Additionally a bain relationship occurs.

Diskussion

The orientation relationship in *steel A* between ferrite and martensite (as-received material) led to the conclusion, that a part of the austenite grains grow with a fixed orientation relationship to the ferrite matrix. It is to assume, that during the intercritical annealing the ferrite in steel A is recrystallized before the austenite formation is finished. Indication about the possible mechanismen of lath martensite formation can be drawn out of the MOOF between martensite laths of the as-received material. The main component of the MOOF, the Bain-relationship, can be understood as a consequence of an austenite-martensite transformation according to Kurdjumov-Sachs with a strong selection of the possible variants of this transformation. Figure 8 shows the MOOF of all possible martensite laths which can be formed out of a single austenite grain if the Kurdjumov-Sachs relation with all the 24 variants is valid. Comparing this MOOF with that of steel A shows, that in the material not all variants of the transformation form neighbouring laths. It must be mentioned that in this representation it cannot be distinguished between the Kurdjumov-Sachs and the Nishijama-Wassermann orientation relationship. All these mechanisms, the orientation relation between ferrite and austenite and the austenite-martensite transformation with its variants, led to a texture of the martensite with high-index components.

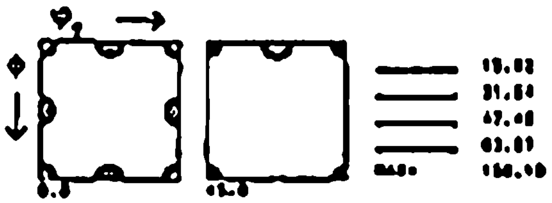

Figure 8: MOOF of all possible martensite laths formed from one austenite grain, if all 24 variants of the Kurdjumov-Sachs relationship are activated

The {111}<uvw>-fibre of the martensite texture after tension deformation is typical for deformed bcc-metals and can be related to a deformation of martensite islands. While in uniphase materials mostly a {111}<110> component is formed in a tensile-test, in this two-phase material a high-index rolling direction occurs. This results from the influence of both phases on each other, that means that the martensite cannot deform as a uniphase material. It must be assumed that not all the texture changes after the tension test are due to the deforming of martensite islands. Also a rigid rotation of martensite particles will result in the change of texture. The part of those islands which will deform can be estimated using the theory of short-fibre composit-materials after Kelly and Tyson (5). This will be only a first approximation since this theory is restricted to unidirectional fibres. Stereological analysis of steel A have shown, that the alignement of the martensite islands is randomly distibuted. Applying this theory to the martensite, it follows that those islands will deform which show an inverse aspect ratio W/L_{crit} less than $(2 \cdot \tau_F)/(\sigma_{F,M})$. With τ_F = shearstress (= $\sigma_F/3$, σ_F = UTS of ferrite) and $\sigma_{F,M}$ = UTS of martensite.

For lath martensite it is $\sigma_{P,M}$ = 550–600 N/mm² and for the ferrite of this alloy it is σ_F = 250 N/mm². These values result in a value for W/L_{crit} of about 0.7. Martensite islands with $W/L_{crit} \leq 0.7$ will deform. Figure 9 shows the frequency of martensite islands over W/L, measured in the longitudinal plane of the as-received and the deformed material. From this it follows that about 90% of the martensite islands could deform. It must be considered that this is only a two-dimensional evaluation of a three-dimensional problem, which gives the lower value for W/L. The rigid rotation of the remaining islands will not give preferred orientations and will weaken the whole texture of the martensite.

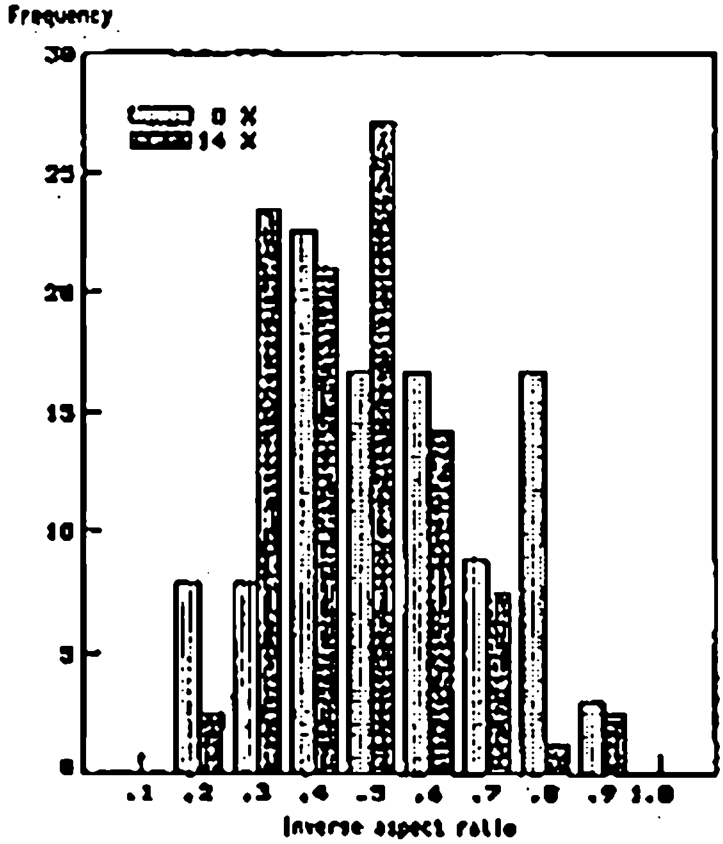

Figure 9: Frequency of the inverse aspect ratio W/L for steel A

In a previous study of texture development of *steel B* (6) it was found that a strong {100}<011> texture was present after hot rolling. By this the development of the {111}<uvw> fibre texture was inhibited which usually forms after cold rolling. This work indicates that this texture component forms within the martensite.

The texture analysis of steel B shows that the martensite forms predominantly with the {100}<011> type orientation. Jones and Walker (7) report that for hot rolled strip rolled in the austenite temperature range, two textures form. Recrystallized austenite has a {100}<001> texture, while deformed austenite has a {123}<412> and {146}<211> texture. Using the Kurdjumov-Sachs orientation relationship it is expected that the lath martensite will form with a {100}<011> texture from the {100}{001} texture. This is confirmed by Jones and Walker and they show that the {211}<011> type textures form from the {123}<412> and {146}<211> texture. The latter is confirmed by Leslie (8) with the addition of the formation of possible {111}<uvw> type textures. Inagaki shows this to be {332}<113> when the austenite is rolled below the recrystallization temperature.

When rolling in the relatively high temperature ranges used in the study of steel B, it is expected that the austenite would dynamically recrystallize during rolling. This would then give the strong {100}<011> textures measured in the martensite. The other weaker textures measured would originate from the austenite that had not fully recrystallized. Comparison of shown ODF indicate this. For 80% reduction, where more deformation of the austenite can be expected, the weak textures are better defined by the continuous orientation spread at the orientations {111}<011> and {211}<102>. In the case of the 20% reduction these orientations are found but the orientation path described is not continuous showing no definite texture development. The only difference due to the different reductions is found in these minor texture components.

Conclusion

The measured orientation relationships in *steel A* led assume that a preferred orientation-ship between ferrite and austenite develops when the austenite is formed during intercritical annealing. The subsequent transformation of the austenite into martensite is near to the Kurdjumov-Sachs relationship. Deforming of the dual-phase steel with 14% elongation in a tension-test led also to a deformation of the lath martensite. The texture is then part of the usual deformation texture of bcc metals.

It was established that the lath martensite in *steel B* forms with a {100}<011> texture after hot rolling. This texture formation is associated with a transformation from recrystallized austenite. For the case of large reduction of 80%, a weak {112} and {111}<uvw> texture forms in the martensite. This is ascribed to limited deformation, which remains in the austenite despite the dynamic recrystallization.

References

1 H. Inagaki, Transformation Textures in Steel, Proc. ICOTOM6, Tokyo, Japan 1981, Iron and Steel Institute of Japan, 149-163.
2 H. Weiland, R. Schwarzer In: Experimental Techniques of Texture Analysis. Ed. H.J. Bunge, DGM Verlagsges. Oberursel (1986), 301
3 H. Weiland, R.A. Schwarzer and H.J. Bunge: Proc. 8th Int. Conf. Textures Materials (ICOTOM 8), Eds. J.S. Kallend und G. Gottstein, Metal. Society, 1988
4 H.J Bunge and H. Weiland: Textures and Microstr., 7 (1988), 231
5 A. Kelly and W.R. Tyson, J. Mech. Phys. Solids 13 (1965), 329
6 L.M. Matthews, G.T. van Rooyen, Proc. 8th Int. Conf. Textures Materials (ICOTOM 8), Eds. J.S. Kallend und G. Gottstein, Metal. Society, 1988, 881-889.
7 A. Jones, B. Walker, Metal Science 1974 vol8, 397-406.
8 Ed. W.C. Leslie, The physical metallurgy of steel, McGraw-Hill, London, 1982, 282